Effects of Forming Route and Heat Treatment on the Distortion Behaviour of Case-Hardened Martensitic Steel type S156

David Easton*, Marcos Perez, Jianglin Huang, Salaheddin Rahimi
Advanced Forming Research Centre, University of Strathclyde, United Kingdom
**david.easton@strath.ac.uk*

Abstract

The distortion behaviour of carburised and fully heat treated Ni-Cr-Mo martensitic steel (S156) has been experimentally evaluated. Dimensional measurements of Navy c-ring distortion coupons during interrupted heat treatment process for parts manufactured from two forming routes, hot forging and machined from as received bar, was performed. Metallurgical analysis was carried out to attempt to relate the observed microstructural characteristics with measured process induced distortion. The carburisation process was found to be the most severe in terms of inducing distortion. It was found that additional heat treatments during the process results in a larger final distortion. Machining parts from forgings results in higher distortions than that of those machined directly from as received bar due to the added thermal processing history. An FE simulation of the carburisation process for a c-ring coupon is presented.

Introduction

Distortion during heat treatment and subsequent processing such as carburisation is a commonly encountered problem when manufacturing steel components for power transmission. The control of dimensional changes during heat treatment is critical, especially in case-hardened components which require large stock removal and a thick case layer, to compensate for high levels of distortion. Power transmission components are often manufactured oversized prior to heat treatments. This allows for stock removal of material to counteract distortion introduced during heat treatment. By adopting heat treatment processes which minimise distortion, the amount of stock removal can be reduced resulting in less machining of the hardened outside layer. The benefit of this is improved tooling and less removal of potentially advantageous hardened and compressively stressed case layer.

The degree of distortion of parts during heat treatment is dependent on many factors including; temperature, time, cooling rate, residual stress, retained austenite, and phase transformation behaviour during heat treatment [1].

In this work the effect of forming process on resulting distortion is assessed. C-ring distortion coupons have been manufactured from two different forming routes including hot forging and machined directly from as received bar stock. The as received bar was in rolled, normalised and annealed condition. The effect of individual heat treatment processes on dimensional change (i.e. distortion) and the variation in distortion behaviour of each forming route has been investigated. Distortion has been measured at various stages of the heat treatment cycle by means of a coordinate measuring machine (CMM) on c-ring coupons. The evolution of microstructure and hardness have been assessed at each stage in an attempt to correlate microstructural and hardness changes with measured differences in distortion of specimens made from forged and as received bar. An FE investigation into carburising induced distortion for the c-ring coupon has also been undertaken and the result is compared with the experimental data.

Methodology

Experimental Procedure
A Navy c-ring type test coupon was used to investigate the evolution of distortion through heat treatment. This specimen type is often used for distortion studies due to the relative simplicity of experimental measurements [2-5].

The geometry of the c-ring coupon are shown in Figure 1. The part has outer diameter of 38mm, inner diameter of 23mm gap width of 4mm and thickness of 8mm. The gap width was machined with tolerance of +/- 0.01mm.

Table 1. Chemical composition S156 steel

Fe	C	Si	M	Cr	Mo	Ni	Cu	Al
Bal	0.15	0.19	0.3	1.16	0.23	3.95	0.09	0.01

All specimens were manufactured from a single batch of S156 bar with 180 mm. The nominal chemical composition of the material is listed in Table 1. A group of specimens were machined directly from the bar in the as-received condition. The specimens were machined with the major faces oriented in the radial plane of the bar. For the other group of specimens, a forging blank was produced by extracting a billet with 130 mm diameter and 80 mm length from the as received bar. This was then forged to 50% reduction at 1150°C using a Schuler AG 2100 tonne screw press located at AFRC, University of Strathclyde.

A total of 18 specimens were produced for each manufacturing route; the as received bar and the as forged billet. The dimensions of the parts were measured in the initial, as-manufactured condition using a Mitutoyo Crystal Apex C CMM with a 1 mm diameter Ruby attached to a Renishaw PH10T probe. Three primary measurements were made; namely inside and outside diameter, and gap width as

illustrated in Figure 1. To increase measurement repeatability, 4 measurements of gap width spanning the thickness of the part were taken for each sample. The mean of these measurements is considered for analyses purposes.

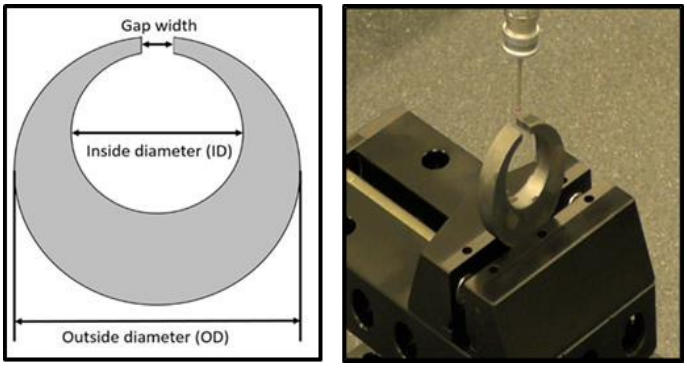

Figure 1. Distortion measurement of c-ring coupon by CMM

Heat Treatment

Dimensional measurements were performed after each stage of the heat treatment process as summarised below:

1. As-manufactured (machined from both as received and as forged)
2. Normalised
3. Carburised and annealed
4. Reheat hardened and sub-zero stabilisation
5. Tempered.

At the end of each heat treatment stage a sample was used for metallurgical analysis.

Normalisation heat treatment was performed at 900°C in a vacuum condition for 1 hour. Carburising was performed in a gas furnace with target case depth of 0.7-0.9mm, followed by annealing at 650°C for 2 hours with air cooling. Hardening was performed via quenching from c. 820°C in oil. Sub-zero treatment was applied to stabilise the retained austenite. Tempering was performed at a temperature of 250°C.

Metallurgical Analysis

For the microstructural analyses, the surface of the c-ring specimens reserved from each heat treatment stage was prepared by conventional grinding and polishing to mirror finished condition. The samples were then chemically etched with a 4% Nital solution. A schematic detailing the areas assessed is shown in Figure 2.

Micro-hardness measurements were conducted using a Zwick/ microhardness testing machine. Measurements in the core material of the c-ring coupons (see Figure 2) were acquired using a diamond shaped Vickers indenter by applying 2000 gf with 10 s delay. Determination of case depth was performed following the traverse method by using Knoop hardness with 500 gr load (HK0.5).

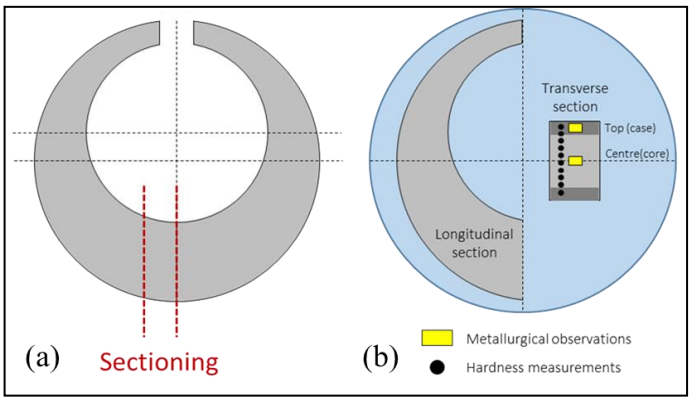

Figure 2. Schematic representation of both the sectioning strategy a), and metallographic analyses for microstructural observations and hardness analysis b), on c-ring specimens

Modelling of Heat Treatment Process

A through process model for steel heat treatment has been developed to improve the understanding of the complex distortion evolution during heat treatment with multiple steps, including furnace heating, carburisation and quenching. Accurate modelling of phase transformation during heat treatment is critical to predict distortion evolution. TTT diagrams, and dilatometry tests have been used to characterise Austenite to Bainite transformation and Austenite to Martensite transformation. The dilatometry tests also provide coefficients of thermal expansion and phase transformation strains, which are critical to provide an accurate prediction of thermally induced residual stress and distortion.

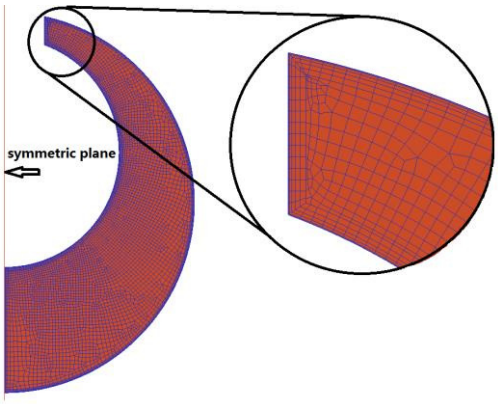

Figure 3. Model setup for C-ring coupon heat treatment.

The setup of finite element model is illustrated in Figure 3. A 2D plane strain model has been developed in DEFORM to simulate distortion evolution during the heat treatment process, which is associated with the mid-plane in the C-ring thickness direction. A symmetric plane is introduced to further reduce the size of the model to a half ring to optimise the computational time. The contact between the ring and the symmetric plane is set by defining the heat transfer and friction coefficients to be zero. To capture the temperature and carbon profile close to the surface accurately, a fine coated meshed was used at the ring surfaces with the finest mesh size of 20 µm. The model consists 5707 elements and 5877 nodes.

The simulated stages during heat treatment includes 3 steps of furnace heating, carburisation and oil quenching. These are summarised as the followings. Annealing step was not simulated.

1. During the furnace heating stage, furnace temperature was set to 900ºC. The heating process lasted for 1 hour followed by 30 minutes soaking. The convection coefficient at the ring surface was set to 0.1 mJ/mm^2/°C throughout the heating stage.
2. In the carburisation process, the workpiece was carburised at 900 ºC for 1 hour at 1.2% carbon potential, followed by diffusion at the same temperature for 30 mins at carbon potential of 1.0%. Then, the furnace cooled down to room temperature.
3. For the quenching process, the workpiece is reheated to 820 ºC and soaked for 45 mins and quenched in oil. In the heating stage, the convection coefficient at the ring surface was set to 0.1 mJ/mm^2/°C. During quenching, the convection coefficient was set to 4.093mJ/mm^2/°C.

Results and Discussion

Distortion

The evolution of distortion during heat treatment of the specimens machined from both the as received bar and forged S156 martensitic steel coupons, is presented in Figure 4. The gap width opening is reported as the metric for distortion. An initial nominal gap width of 4mm was machined by EDM. A key for the order of heat treatment processes is included in each Figure. Measurement uncertainty has been reported as one standard deviation in measured gap widths for all samples in a given population (i.e. all samples from both the as received bar and forged billet).

The distortion measurements presented were taken in the as-manufactured condition, as-carburised and annealed, as-hardened and stabilised, and as-tempered condition. Normalising heat treatment was not applied here, and is discussed in the subsequent section.

Overall, distortion was found to be larger in magnitude for the C-ring coupons manufactured from the forged billet compared to that measured on the coupons machined from the as received bar. This is observed by considering the final measured gap widths in Figure 4. The initial, as-manufactured gap widths are similar in size, ≈ 4mm. During the heat treatment process, both conditions experienced distortion in the form of gap width opening. The final distortion of the specimens from forged billet was ≈ 0.45mm compared with 0.32mm for those machined from as received bar. The differential in distortion measured for specimens from both as received bar and as forged billet increases with each heat treatment process applied.

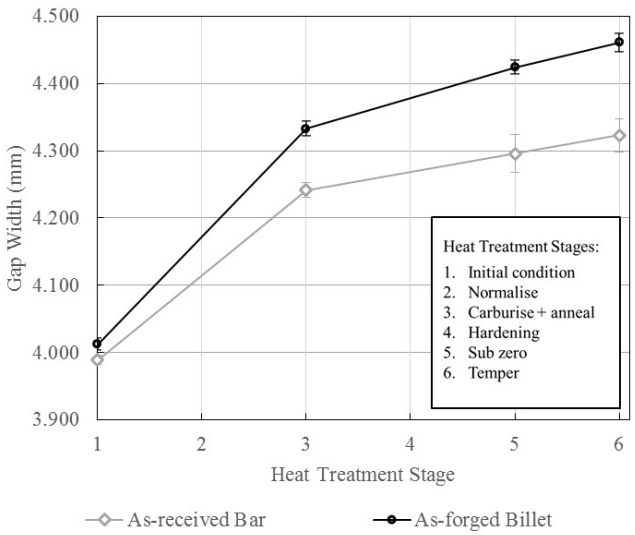

Figure 4. Measured distortion of C-ring coupons machined from both the as received bar and as forged S156

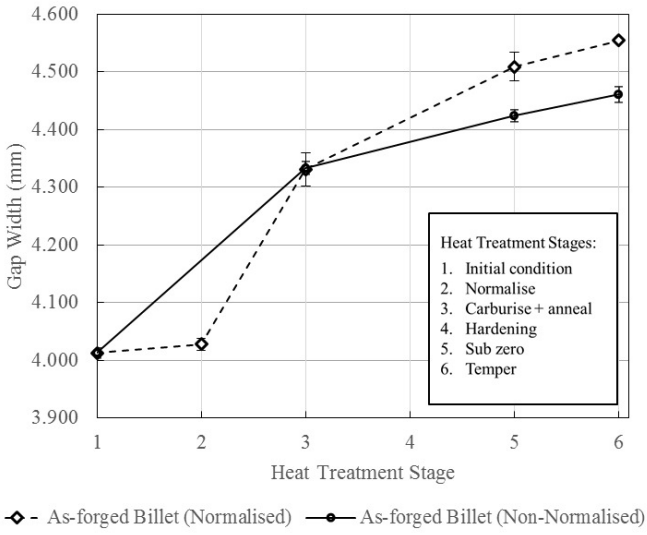

Figure 5. Effect of normalising heat treatment on distortion in C-ring coupons machined from as forged billet

The effect of applying a normalising heat treatment prior to the case hardening process was investigated. The measured distortion on specimens made from the as forged billet in the normalised and non-normalised conditions are presented in Figure 5.

A higher degree of distortion was observed in the normalised parts compared with those that were omitted from the normalisation and annealing process. Distortion is often caused by relaxation of residual stresses during normalisation or stress relieve processes [1]. However, the increase in distortion is not immediately apparent following normalisation treatment as only a small degree of gap width opening was observed. After carburising and annealing the two conditions

exhibit essentially identical degrees of distortion. However, upon subsequent treatments, namely hardening, sub-zero and tempering, there is a marked increase in distortion for normalised parts compared with those non-normalised.

Previous studies into distortion of martensitic steel coupons found that increasing the number of heat treatment processes a results in increased tendency for distortion [6]. This trend was clearly confirmed in the trials presented here. When comparing the three conditions presented for specimens: from- as received bar (non-normalised), from-as forged billet (non-normalised) and from-as forged (normalised), a clear trend develops. The highest distortions measured for normalised specimens from the as forged billet can be due to the two additional heat treatments they are subjected to, compared to the non-normalised specimens from the as forged billet. A bigger variation in distortion is found between the normalised specimens from the forged billet and those from the as received bar, with final gap width opening of 0.55mm and 0.32mm, respectively. This suggests that the number of thermal processes applied to a part correlates directly with increasing distortion in the final part.

The relative effect of each heat treatment process on the final, cumulative distortion following heat treatment has been assessed. The change in gap width measured, i.e. distortion observed, for the conditions discussed is shown in Figure 6.

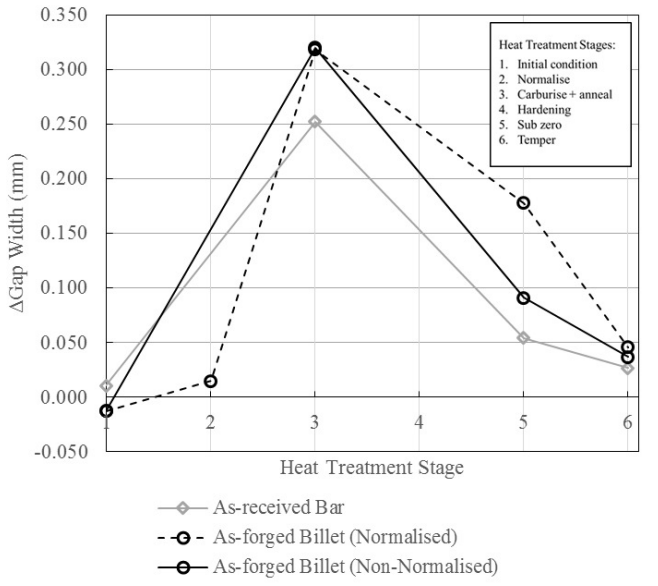

Figure 6. Contribution of each heat treatment process on *cumulative distortion (Δ gap width)*

The carburisation process was shown to have the most influential impact on distortion of the martensitic steel coupons. During this process there are multiple factors which can be attributed to causing the permanent dimensional change. Carburising is performed in the austenite condition, so a full martensite-austenite and subsequent austenite-martensite transformation occurs and is known to influence distortion [1]. However full transformation also occurs during normalising and hardening, so there are clearly additional factors to be considered. One of which is the introduction of carbon to the part, resulting in a carbon rich case layer. The volumetric change due to carbon addition, combined with a change in carbon dependant transformation behaviour is likely to influence the increased levels of distortion after this process.

The normalising process can be clearly seen to have little immediate effect on distortion (see Figure 6), but is clearly influential on the final distortion experienced by the martensitic steel C-ring specimens (see Figure 5). The effects of tempering on distortion are minimal, largely due to the absence of austenitic transformation present.

As carburisation was found to be the most significant contributor to distortion behaviour, this process was selected for the focus of the FE analysis study of heat treatment induced distortion of S156 steel, presented in the Modelling section.

Micro-Hardness

In carburised components subjected to cyclic loading, in addition to fatigue resistance, hardness is a commonly measured property used as a quality control parameter to assess the carburising response and to establish case depths. For example, core hardness of teeth is an important parameter that determines the strength of a gear tooth [7].

The evolution of the mean micro-hardness (HV2) measured on the core of the C-ring specimens at different stages for the two manufacturing routes (as received bar, as forged billet) is plotted in Figure 7. The hardness of C-ring specimens machined directly from the as-received bar is 227 HV2. The hardness increases up to 325 HV2 for the specimens made from the billets in as-forged condition. This higher value is associated to the bainite transformation during air cooling from forging temperatures ($T >> A_{c3}$). A very similar value (331 HV2) is obtained for the specimen from the as forged billet in as-normalised condition. Note that the normalising treatment was not applied on the C-ring specimens machined directly from the as received bar.

In as-carburised condition plus subsequent annealing treatments), core hardness values were measured to be in the range of 243-249 HV2. In as-hardened condition plus sub-zero treatment, the hardness increases to a range of 441-454 HV2, which is associated to untempered martensite. In the final step(i.e. as-tempered condition), the core hardness drops from 441-454 HV2 range to 423-434 HV2 range as a result of the tempering treatment at 250 ˚C. These results imply a consistent hardness evolution across the C-ring specimens machined from both the as received bar and as forged billet.

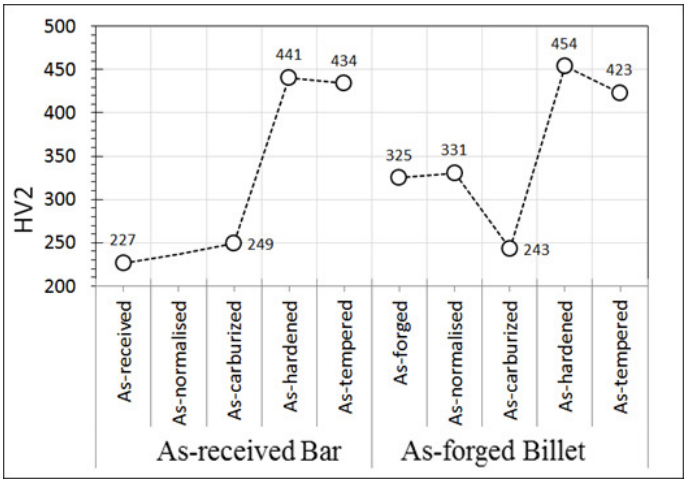

Figure 7. Core hardness (HV2) evolution of the C-ring specimens

The case hardness of the C-ring specimens manufactured from both types of initial materials (i.e. ad received and as forged) was also analysed at three different stages of as-carburized, as-hardened and as-tempered conditions. The case depth was estimated based on the core hardness + 120 points HV method in as-hardened and as-tempered conditions. This method for defining case depth was that utilised by the commercial heat treatment company used for this research. Figure 8 plots the case hardness results from the C-ring specimens in as-carburised (Figure 8.a), as-hardened ((Figure 8.b) and as-tempered conditions (Figure 8.c). The horizontal dashed lines corresponds to the threshold hardness for case depth measurement ($HK0.5_{CASE}$).

From Figure 8, very similar hardness profiles were found in C-ring specimens manufactured from both the as received bar and as forged billet. Note that the curves of hardness profiles are almost overlapped for all the three conditions. In as-hardened condition, a consistent case depth of about 1.1 mm was measured in the C-ring specimens machined from both the as received bar and as forged billet. In other words, a homogenous case depth was obtained in all the C-ring specimens regardless of the initial material state (i.e. as received or as forged).

In the as-tempered condition (Figure 8.c), a remarkable drop in hardness was measured. The maximum hardness close to the carburised surface drops from 760 HV2, in as-hardened condition (Figure 8.b), to 650 HV2 in as-tempered condition (Figure 8.c). The case depth is also strongly affected by the tempering treatment, reducing from 1.1 to 0.6 mm for the as-hardened and as-tempered conditions, respectively. It seems that for the tempering treatment at 250 ˚C, the core + 120 HV method gives erroneously low case depth results.

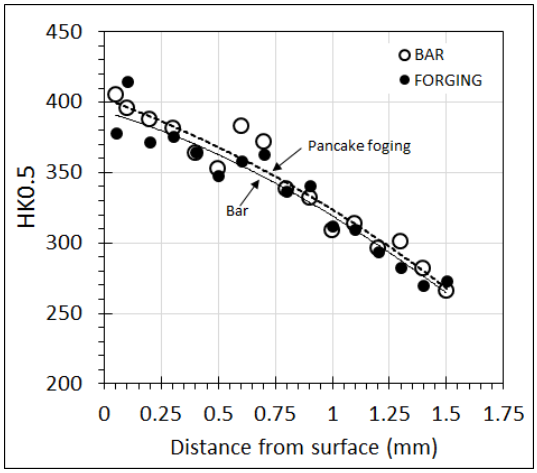

a) As-carburised condition

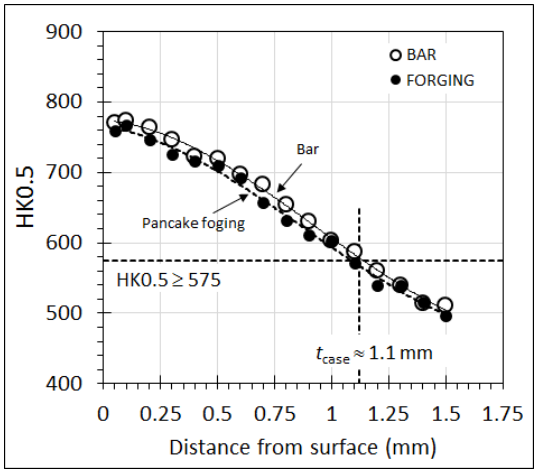

b) As-hardened condition

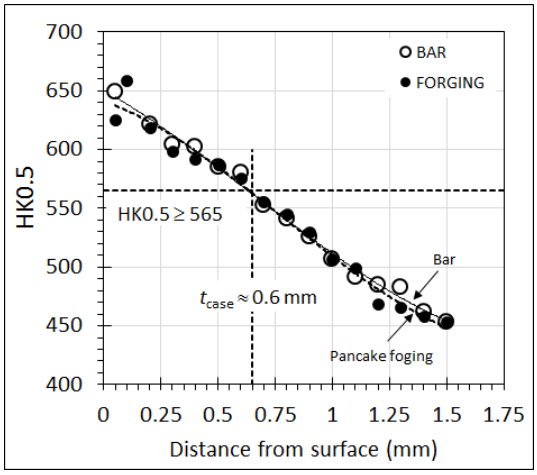

c) As-tempered condition

Figure 8. Case hardness (HK0.5) evolution of the C-ring specimens

Microstructural Analysis

Figure 9 shows the radial cross-sections of the C-ring specimens etched with 4% Nital. A change in the etching response is observed after each single heat treatment cycle (i.e. normalising, carburising, hardening and tempering). From these figures, the presence of the case layers is also inferred at both top and bottom surface. For a given heat treatment, a

consistent etching response was found across both manufacturing routes.

An interesting feature observed in Figure 9 is the banding structure observed in the C-ring specimens in both the as-received and as-forged conditions. This microstructural alignment is reserved after the subsequent heat treatments which often cause phase transformations. The observed microstructural alignments are associated with the presence of micro-segregation bands in the as-supplied material (S156 bar), originally oriented in the rolling direction, and not in the direction of grain flow.

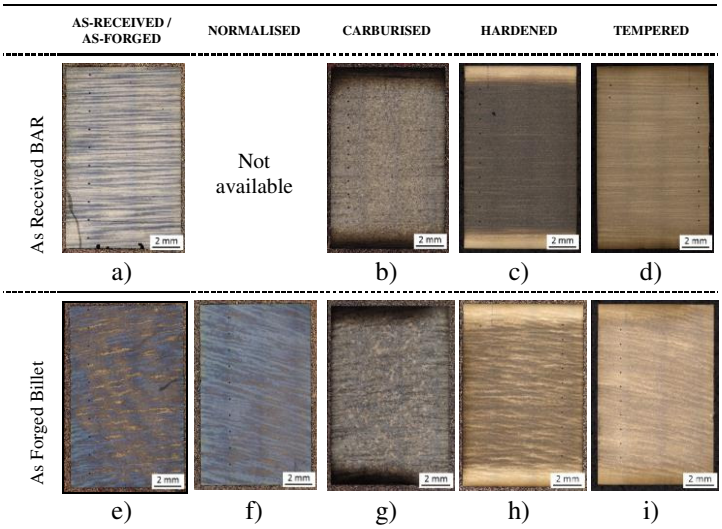

Figure 9. Radial cross-sections of S156 C-ring specimens etched with 4% Nital.

Figure 10 shows the microstructural evolution in the C-ring specimens from both sources of materials at core positions in as-carburised, as-hardened and as-tempered conditions. No apparent microstructural differences were observed across both manufacturing routes. A significant grain refinement is observed after the hardening treatment. This can be explained by both the additional phase transformation and the change from bainitic structures in as-carburised condition (Figure 10.a & b), to quenched/tempered martensite in as-hardened condition (Figure 10.c & d) and (Figure 10.e & f), with a higher density of low angle boundaries in the interior.

Figure 11 show the martensitic microstructure of the C-ring specimen in the as-hardened condition from the as forged billet. A very fine distribution of carbides in the interior of the lath structure was found. This phenomenon is referred to as auto-tempering, and occur in the first-formed martensite, i.e. the martensite formed near Ms, which has the opportunity of tempering during the remainder of the quench [8].

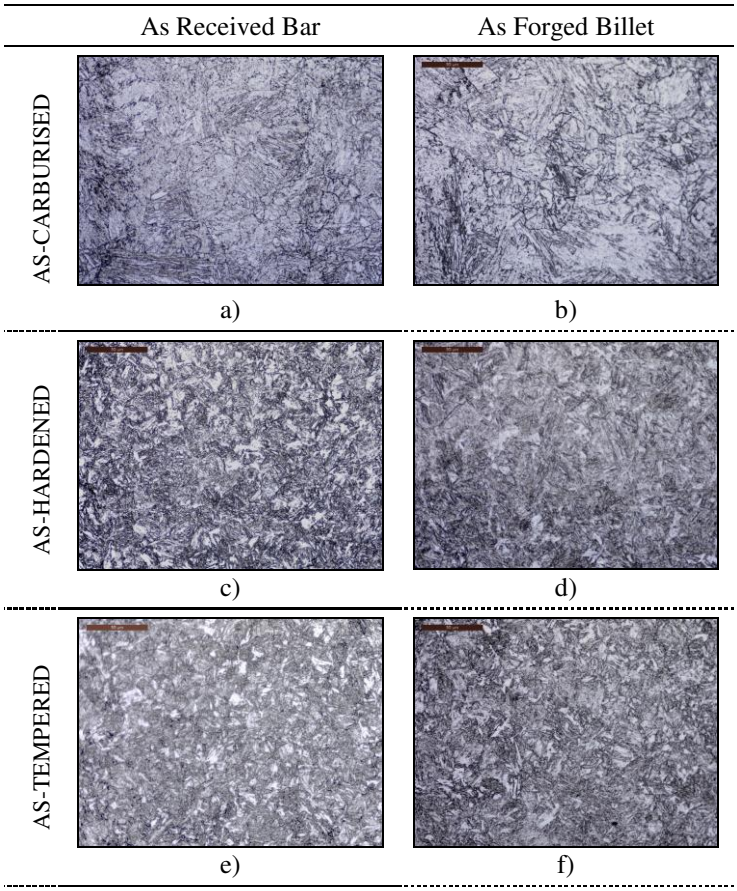

Figure 10. Optical micrographs of C-ring specimens at core positions.

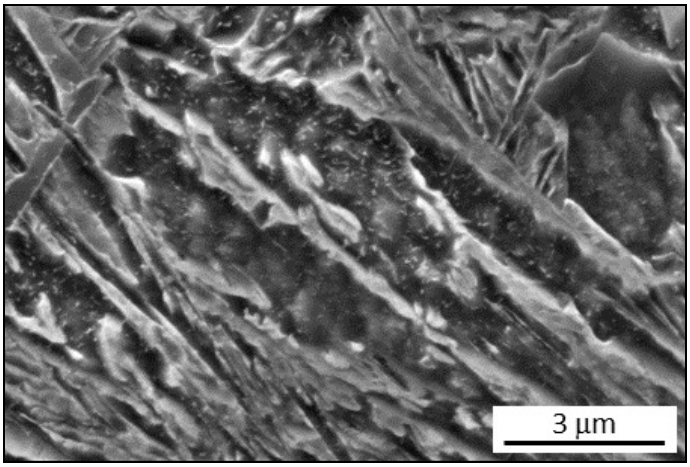

Figure 11. A SEM micrograph of a C-ring specimen made from the as forged billet at core positions in as-hardened condition

Figure 12 shows the microstructural evolution of C-ring specimens at case positions for both routes in as-carburised, as-hardened and as-tempered conditions. No apparent microstructural differences were observed across both manufacturing routes. In as-carburised condition (Figure 12 & b), continuous carbide networks fully decorating the prior

austenite grain boundaries can be observed, especially close to the carburised surface. Further work was conducted by using SEM to analyse the presence of such carbides in more details.

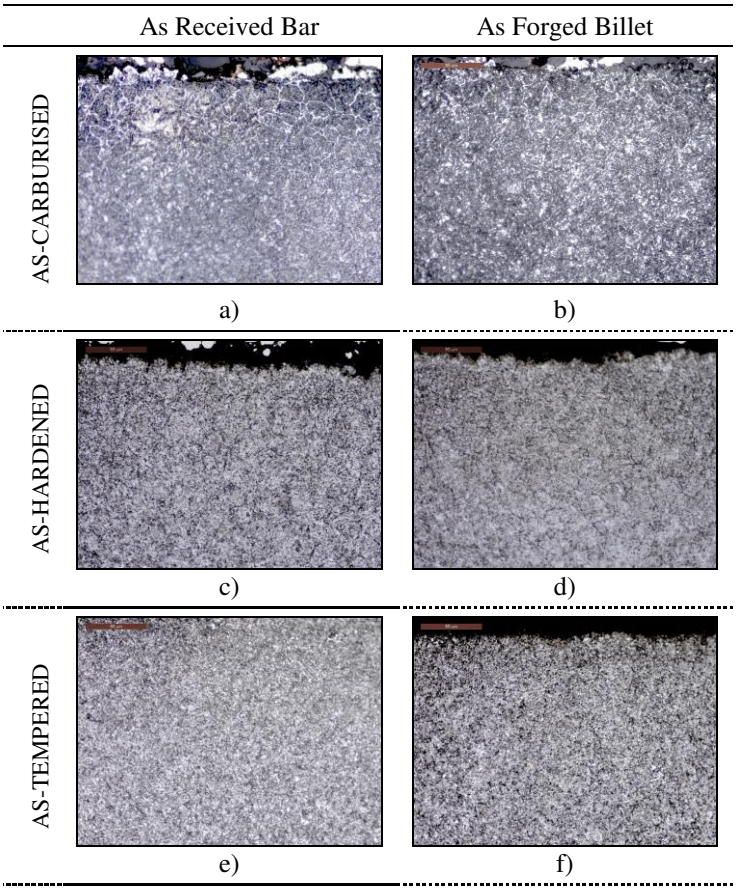

Figure 12. Optical micrographs of C-ring specimens at case positions.

Figure 13 shows the microstructural evolution of C-ring specimens at case positions, close to the carburised surface, after the carburizing, hardening and tempering treatments. In the as-carburised condition, continuous carbides networks along the prior austenite grain boundaries were found (Figure 13.a). In the as-hardened condition, it is obvious that the hardening treatment has resulted in firstly, partial dissolution and globularisation of the coarse carbides formed during gas carburising at prior austenite grain boundaries, and secondly, subsequent precipitation of fine globular carbides within the plate martensite (see Figure 13.b). A bimodal carbides distribution is observed. No apparent differences in carbides distribution were observed between the specimens in the as-hardened (Figure 13.b) and the as-tempered conditions (Figure 13.c).

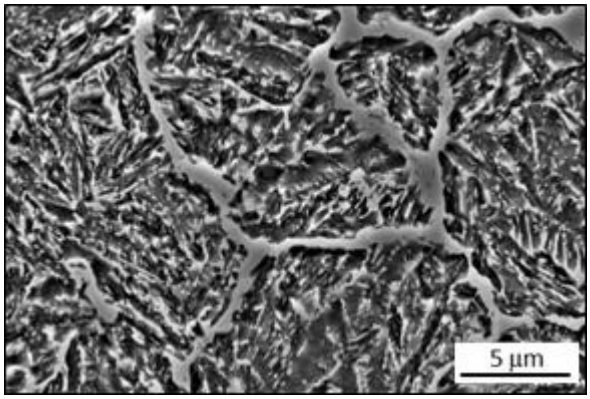

a) As-carburised condition

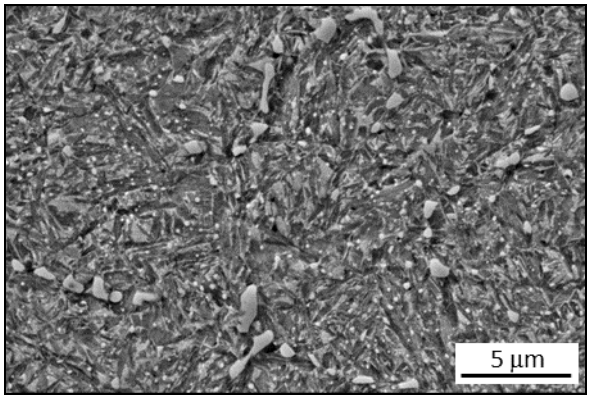

b) As-hardened condition

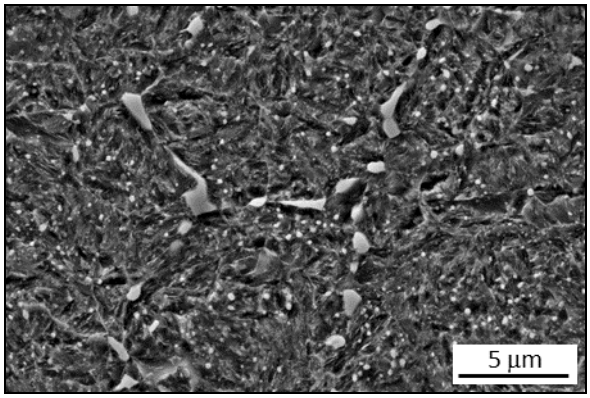

c) As-tempered condition

Figure 13. SEM micrographs of C-ring specimens made from the as forged billet at case positions

Modelling

Figure 14 shows the predicted carbon content distribution after carburisation process. The peak carbon content at the ring surface is close to 1.0%, which is relevant to the carbon potential level during soaking before finishing the carburisation process. A line probing results shows the carbon penetrating depth is close to 1 mm. Since the carbon profile has not been measured in this work, a direct comparison with experimental results is not applicable. However, the case depth estimated in in Figure 8 through hardiness measurement indicates a reasonable correlation between the carbon penetration and case depth.

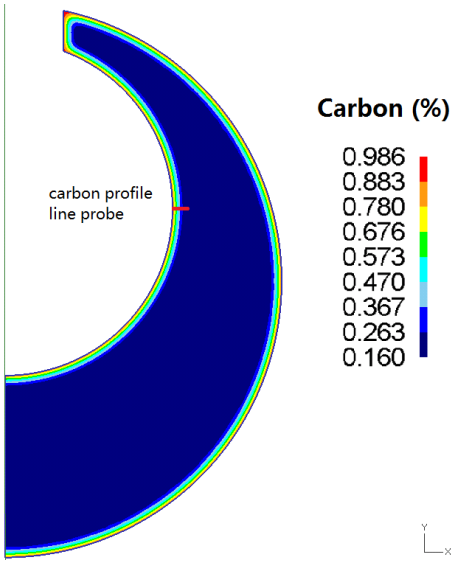

(a) Carbon distribution contour

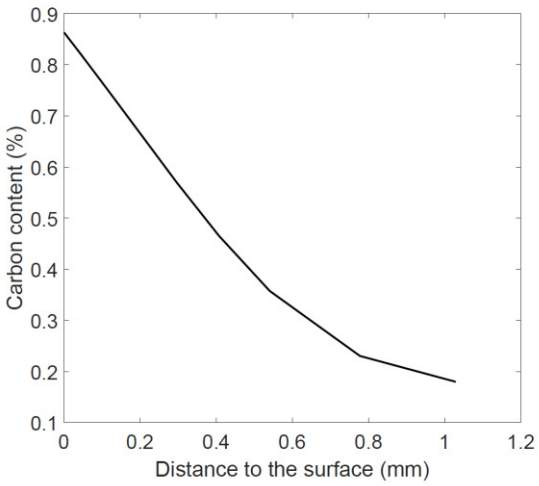

(b) Carbon profile distribution (line probe)

Figure 14 Predicted carbon distribution after carburisation.

For realistic simulations of phase transformation and distortion, an accurate material data of phase transformation and phase dependent material properties are required, which were made using the JMatPro software [9]. Figure 15 shows the predicted evolution of martensitic transformation. It can be seem that martensitic transformation start from the inside of the thin section in the ring. The increase carbon in the case delays the martensitic transformation. However due to the rapid cooling of this small C ring part, Bainite transformation was found to be negligible. At the end of quenching process, around 10% of retained austenite was found in a thin layer close the C ring surface.

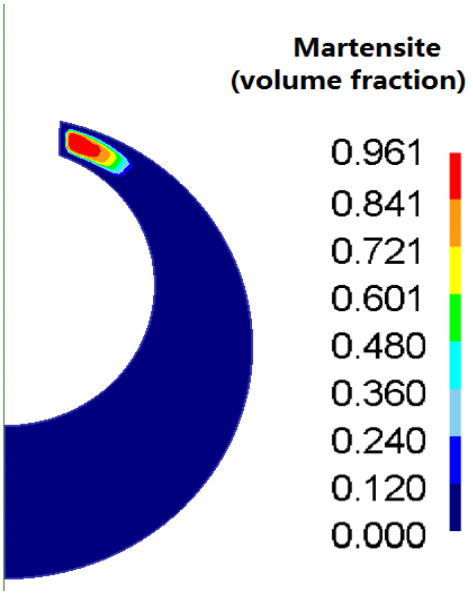

(a) Volume fraction of Martensite (quench t=2s)

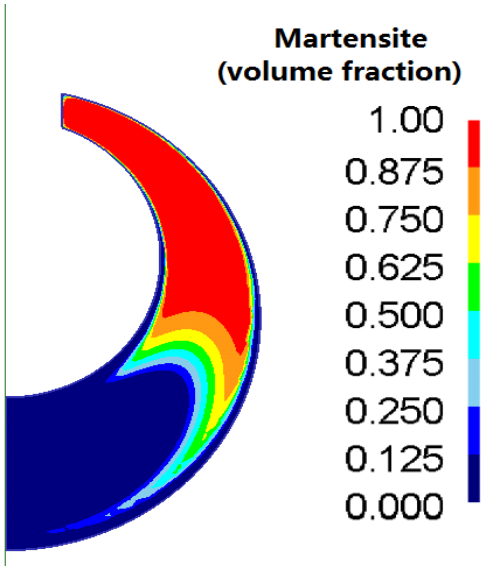

(b) Volume fraction of Martensite (quench t=10s)

Figure 15 Predicted evolution of Martensitic transformation.

Figure 16 shows the final displacement after quenching. Although this displacement contour cannot be compared with experimental, the displacement in horizontal direction (X direction) as shown in Figure 17 is correlated to the distortion measurement reported in Figure 4 and Figure 5 by measuring the gap opening in the C ring samples. The predicted distortion is in a reasonably good agreement with the experimental measurements.

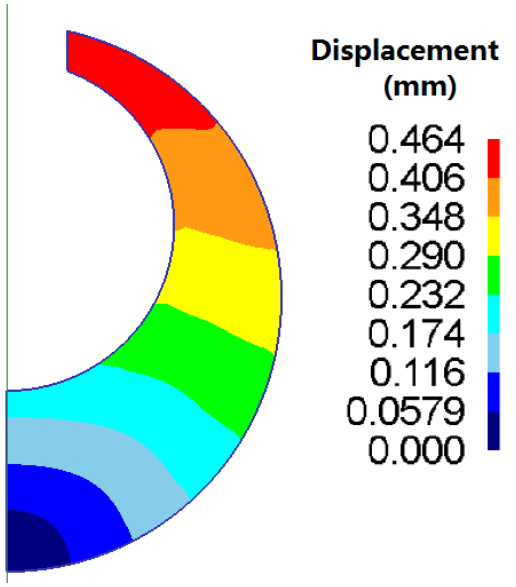

Figure 16 Predicted displacement after quenching.

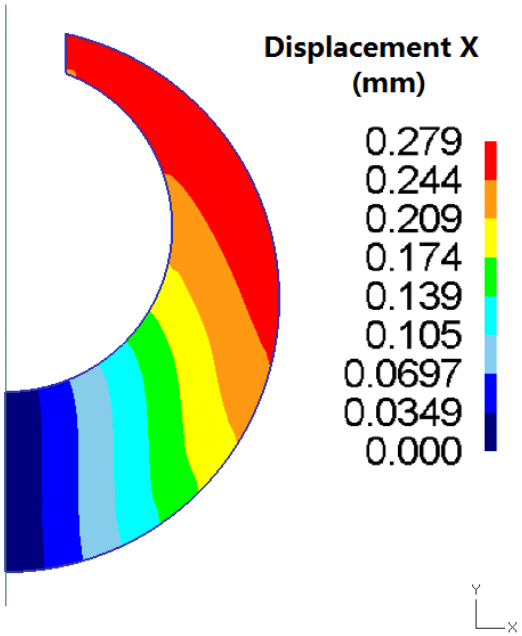

Figure 17 Predicted displacement in the horizontal direction (X direction) after quenching, correlating to gap opening of C ring.

Conclusions

- Level of heat treatment induced distortion is strongly dependent on the thermal history of the steel. A correlation between increased heat treatment processes and increased final geometrical distortion was observed. A population of specimens were subjected to an additional heat treatment prior to carburisation, namely normalising and annealing, which experienced more distortion than those non-normalised with identical processing history.
- After completion of the heat treatment process a larger level of distortion was observed in specimens made from as forged billet compared to those machined directly from the as received bar. It is postulated that the additional heat treatment processes, and therefore austenisation and subsequent martensitic transformation of the as forged specimens is the principal factor resulting in higher distortion.
- The heat treatment process which induces significant distortion in case-hardened martensitic steel is carburisation. Although normalising treatment was found to have an ultimately stronger impact on distortion behaviour, this is not apparent immediately following both normalisation and carburisation processes.
- A consistent etching response, microstructural and hardness evolutions were found across C-ring specimens machined from both the as received bar and as forged billet. No significant differences were found which can provide a clear explanation about the larger distortion detected in C-rings manufactured from the as forged billet. In both the as-received and as forged conditions, a strong microstructural directionally was observed that is likely to be the alignment of micro-segregation bands with rolling direction. Such directionality is reserved along the whole heat treatment cycles.
- A through process model has been developed to investigate the distortion evolution during the heat treatment process. The current model only considers 3 steps including the furnace heating, carburisation and quenching processes. Predicted case depth and distortion are in reasonably good agreement with the experimental measurements.

Acknowledgments

This research was carried out with financial support from Aerospace Technology Institute and Rolls-Royce as part of the MAMOTH PGB programme. The authors of this work would like to thank: Dr. Christopher Watson from Rolls-Royce plc. and Dr. Zhanli Guo from Sente Software Ltd., UK (JMatPro) for providing S156 material data, for the simulation work.

References

[1] L. Canale and G. E. Totten, "Overview of distortion and residual stress due to quench processing. Part I: factors affecting quench distortion," International Journal of Materials and Product Technology, vol. 24, pp. 4-52, 2005.

[2] C. Nan, D. O. Northwood, R. J. Bowers, X. Sun, and P. Bauerle, "The use of navy C-ring specimens to study distortion in ferritic nitrocarburized 1010 steel," in WIT Transactions on Engineering Sciences, 2009, pp. 13-25.

[3] M. Manivannan, D. O. Northwood, and V. Stoilov, "Use of Navy C-rings to study and predict distortion in heat treated components: Experimental measurements and computer modelling,"

International Heat Treatment and Surface Engineering, vol. 8, pp. 168-175, 2014.

[4] A. D. da Silva, T. A. Pedrosa, J. L. Gonzalez-Mendez, X. Jiang, P. R. Cetlin, and T. Altan, "Distortion in quenching an AISI 4140 C-ring – Predictions and experiments," Materials & Design, vol. 42, pp. 55-61, 2012.

[5] N. Cyril, B. Cyrille, L. Stéphane, T. Mihaela, and B. Régis, "Comparison of experimental and simulation distortions of quenched C-ring test parts," International Journal of Material Forming, vol. 2, p. 263, 2009.

[6] G. Blake, "The effects of pre rough machine processing on dimensional distortion during carburizing," American Gear Manufacturers Association.

[7] J. R. Davis, Gear Materials, Properties, and Manufacture: ASM International, 2005.

[8] H. Bhadeshia and R. Honeycombe, "Chapter 5 - Formation of Martensite," in Steels: Microstructure and Properties (Fourth edition), ed: Butterworth-Heinemann, 2017, pp. 135-177.

[9] Z. Guo, N. Saunders, J. P. Schillé, and A. P. Miodownik, "Material properties for process simulation," Materials Science and Engineering: A, vol. 499, pp. 7-13, 2009/01/15/ 2009.